residue was partitioned between EtOAc and H_2O. The EtOAc layer was washed successively with ice-cold 1 N HCl (2 × 50 mL), H_2O, saturated aqueous $NaHCO_3$, and saturated aqueous NaCl. Drying (Na_2SO_4) and solvent evaporation left a gum (3.3 g), which was chromatographed on a silica gel column (40 × 2.5 cm) with 2.5% MeOH in $CHCl_3$ followed by 5% MeOH in $CHCl_3$ as the eluents. TLC homogeneous fractions (R_f 0.82, silica gel, 4:1 $CHCl_3$–MeOH) were pooled and evaporated, and the residue was recrystallized from MeCN: yield 1.04 g (46%); mp 123–126 °C; IR (KBr) ν 3420, 2950, 1650 cm^{-1}; NMR ($CDCl_3$) δ 1.03 [s, 28 H, 2 $(Me_2CH)_2Si$], 4.03 (m, 2 H, C_3-H and C_4-H), 4.7 (m, 1 H, C_2-H), 5.36 (m, 1 H, C_1-H), 8.2 (s, 1 H, C_5-H). Anal. ($C_{22}H_{39}N_5Si_2O_5$) C, H, N, Si.

A more polar fraction (R_f 0.48, silica gel, 4:1 $CHCl_3$–MeOH) was recovered from the column. Solvent evaporation left a gum (0.8 g) that, on treatment with 1 M tetra-*n*-butylammonium fluoride in THF and with ion-exchange chromatography on Dowex 50W-X8 (H^+) as described below, gave unchanged **1** (0.34 g, 25% recovery). The yield of **2** after correction for this recovery was 61%. The chromatographic behavior of the silylation by-product and its subsequent conversion to formycin A in the presence of fluoride ion suggest that it is a noncyclic 5′- and/or 3′-monosilyl derivative.

7-Amino-3-[3′,5′-*O*-(1,1,3,3-tetraisopropyl-1,3-disiloxanediyl)-2′-(phenoxythiocarbonyl)-β-D-ribofuranosyl]pyrazolo[4,3-*d*]pyrimidine (4). Phenoxythiocarbonyl chloride (400 μL, 2 mmol) was added from a dry syringe to a solution of **3** (968 mg, 1.9 mmol) and 4-(*N*,*N*-dimethylamino)pyridine (1.85 g, 15.2 mmol) in anhydrous MeCN (50 mL). Stirring was continued at room temperature for 24 h, the solvent was removed by rotary evaporation, and the crude product was partitioned between EtOAc and H_2O. The EtOAc layer was washed as in the preceding experiment, the solvent was evaporated, and the crude product (1.38 g) was chromatographed on silica gel with 1:1 $CHCl_3$–MeCN as the eluent. Pooled TLC homogeneous fractions (R_f 0.46, silica gel, 9:1 $CHCl_3$–MeOH) were evaporated, and the residue was recrystallized from MeCN: yield 0.8 g (66%); mp 142–145 °C; IR (KBr) ν 3420, 3200, 1650 (C=N), 1210 (C=S) cm^{-1}; NMR ($CDCl_3$) δ 1.1 [s, 28 H, 2 $(Me_2CH)_2Si$], 4.15 (m, 2 H, C_3-H and C_4-H), 4.93 (m, 1 H, C_2-H), 5.7 (m, 1 H, C_1-H), 7.3 (m, 5 H, aromatic), 8.3 (s, 1 H, C_5-H); mass spectrum 646 (M + 1), 510 (M − C(=S)OC_6H_5), 492 (510 − H_2O), 376 (510 − base). Anal. ($C_{29}H_{43}N_5Si_2O_6S$) C, H, N, S.

7-Amino-3-(2′-deoxy-β-D-ribofuranosyl)pyrazolo[4,3-*d*]pyrimidine (2). Hexamethyldisilazane (50 mL) and $(NH_4)_2SO_4$ (25 mg) were added to **4** (484 mg, 0.75 mmol), and the reaction mixture was heated to reflux for 1 h. After evaporation under reduced pressure, the crude trimethylsilyl derivative was dissolved in dry redistilled toluene (50 mL) and α,α′-azobisisobutyronitrile (60 mg, 0.75 mmol) and tri-*n*-butyltin hydride (3 mL, 16.9 mmol) were added. The solution was purged with O_2-free N_2 for 0.5 h and then heated at 75 °C for 4 h, with TLC monitoring to ensure that reduction was complete. Deprotection was performed directly by adding 2 mol equiv of tetra-*n*-butylammonium fluoride in THF (1.5 mL of a 1 M solution) and heating at 75 °C for another 2 h. The solvent was evaporated under reduced pressure, and the residue was partitioned between Et_2O and H_2O. The H_2O layer was concentrated to a small volume and applied onto a column of Dowex 50W-X8 (H^+) resin. The column was washed first with H_2O (2 L) and then 15% NH_4OH. Fractions containing the product (TLC) were combined and purified further by preparative TLC on silica gel using 4:1 $CHCl_3$–MeOH as the developing solvent: yield 100 mg (53%); mp 163–166 °C; R_f 0.3 (silica gel, 4:1 $CHCl_3$–MeOH); IR (KBr) ν 3420, 2930, 1650, 1520, 1400 cm^{-1}; UV (MeOH) λ_{max} 229 nm (ϵ 5932), 293 (8898), 304 (6471); NMR (CD_3OD) δ 2.3–2.6 (m, 1 H, C_2-H), 3.57 (d, 1 H, C_5-H_a), 3.8 (m, 1 H, C_5-H_b), 4.15 (m, 1 H, C_4-H), 4.5 (d, 1 H, C_3-H), 5.6 (dd, 1 H, C_1-H), 8.2 (s, 1 H, C_5-H); mass spectrum 252 (M + 1). Anal. ($C_{10}H_{13}N_5O_3 \cdot 0.4CH_3OH \cdot 1.5H_2O$) C, H, N.

Cytotoxicity Assays. The properties and growth characteristics of S49 murine lymphoma cells and of their kinase-deficient mutants have been described previously.[19,22] Cell growth experiments were performed with suspensions of log phase phase cells (initial density 10^5/mL) in multiwell microtiter plates, using Dulbecco's modified Eagle's medium supplemented with 10% heat-inactivated horse serum and 2 mM L-glutamine. Drugs were dissolved in H_2O at pH 7.5. Cells were counted after 72 h with a Coulter Counter Model ZB1, and cell growth was expressed as a percent of the growth in untreated control cultures. The drug concentration giving a 50% reduction in growth (IC_{50}) was determined from the dose–response curve. Duplicate experiments showed good reproducibility (see Table I).

Acknowledgment. This work was supported in part by Grant CA31737 from the National Cancer Institute, DHHS. The authors are grateful to Dr. Vernon Rheinhold, Department of Nutrition, Harvard School of Public Health, for his help in obtaining mass spectra.

Registry No. **1**, 6742-12-7; **2**, 96893-70-8; **3**, 87791-95-5; **3** (2′-trimethylsilyl derivative), 96807-07-7; **3** (2′-deoxy derivative), 96807-08-8; **4**, 96807-06-6; phenoxythiocarbonyl chloride, 1005-56-7.

(22) Ullman, B.; Cohen, A.; Martin, D. W., Jr. *Cell* **1976**, *9*, 205.

Correlation of Structure and Activity in Ansamycins: Structure, Conformation, and Interactions of Antibiotic Rifamycin S

Satish K. Arora

Drug Dynamics Institute, College of Pharmacy, The University of Texas at Austin, Austin, Texas 78712.
Received September 26, 1984

The crystal and molecular structure of the DNA-dependent RNA polymerase inhibiting antibiotic rifamycin S ($C_{37}H_{45}O_{12}N$) as a dihydrate has been determined, and the conformation necessary for activity has been correlated with those of other active rifamycins. The orthorhombic unit cell, space group $P2_12_12_1$ with dimensions of a = 13.010 (2), b = 14.236 (2), c = 20.571 (4) Å, contains 4 molecules. The structure was solved by a combination of vector search and direct methods and refined anisotropically to an R factor of 0.048 for 2855 reflections. The conformation of the *ansa* chain differs from those of rifampicin and rifamycin B but resembles that of rifamycin SV at the joining points, C(2) and C(12), of the *ansa* chain to the naphthoquinone chromophore. The middle part of the *ansa* chain, which is essential for its activity against the enzyme, has the same conformation as other active rifamycins. The effect of the 3-substitution on the *ansa* chain conformation is that the carboxyl (C(15)=O) group wings around the N–C(16) direction, depending upon the electronegativity of the 3-substituent. The hydrogen bonding involves O(1), O(2), O(8), O(9), O(10), and the water molecules. A possible four-stage model for the interaction of the rifamycins with the enzyme DNA-dependent RNA polymerase has been speculated.

Rifamycins are naphthalenic ansamycins, which are produced from *Streptomyces mediterranei*.[1] These antibiotics are active against a large variety of organisms, including bacteria, eukaryotes, and viruses. They have

0022-2623/85/1828-1099$01.50/0

shown antitumor activity[2] but at present are mainly used for the treatment of tuberculosis. Their antimicrobial activity is due to the inhibition of bacterial DNA-dependent RNA polymerase (DDRP).[3,4] Many attempts have been made to rationalize the structure–activity relationships involved in this inhibition.[5-10]

Until recently, all of the crystal structure studies of rifamycins have been made on molecules that contained either 3- or 4-substituents, e.g., rifampicin (RIFAMP),[11] rifamycin B *p*-iodoanlide (RIFAB),[5] and 3-carbomethoxyrifamycin S (CMRS),[12] or those with changes in the *ansa* chain (thus inactive), e.g., tolypomycinone (TOLYPO),[13] rifamycin S iminomethyl ether (RIFASIME),[9] and cyclized rifamycins SV (CYRIFASV).[10] Recently, the structure of the sodium salt of rifamycin SV was determined by the author.[8] The present study represents the first structure of an active rifamycin (rifamycin S is the oxidized form of the redox pair involving rifamycins S and SV) in its natural form (no substitution or metal).

Experimental Section

Data Collection. Rifamycin S was kindly provided by Drs. Muller and Scheibli of Ciba-Geigy, Basel. Crystals suitable for single-crystal studies were obtained by slowly evaporating an aqueous methanol solution of the compound. A crystal measuring 0.3 × 0.2 × 0.2 mm was used for the measurement of cell constants and data collection. The crystals belonged to the orthorhombic space group $P2_12_12_1$ with cell dimensions of a = 13.010 (2) Å, b = 14.236 (2) Å, c = 20.571 (4) Å, Z = 4, D_{measd} = 1.245 g cm^{-3} (CCl_4/petroleum ether), D_{calcd} = 1.242 g cm^{-3}, fw = 713.48, V = 3810.0 Å^3. The intensities of 3931 unique reflections with $2\theta \leq 50°$ were measured at room temperature with Mo K_α radiation (λ = 0.710 69 Å) on a Syntex $P2_1$ diffractometer equipped with a graphite monochromator, using a θ–2θ scan technique, a variable scan rate (2.0–29.3°/min), a scan range of 2.0°, and a background-to-scan ratio of 0.5. A total of 2855 reflections greater than 3σ(I) were considered observed. Three check reflections were monitored every 100 reflections, and no significant deterioration in the check reflections was observed. Lorentz and polarization corrections were applied to the data. The unit cell parameters were obtained by the least-squares fitting of settings of 15 reflections having a 2θ range of 10–25°.

Structure Determination and Refinement. Attempts to solve the structure of the direct methods program MULTAN 78[14] met with failure initially. Finally, the orientation of the chromophore was obtained by the Patterson search method. When this orientation was put into the direct-methods program, the E map (390 E values ≥1.5) revealed 45 of 50 non-hydrogen atoms in the molecule. The remaining five non-hydrogen atoms and water oxygens were located from the difference Fourier map.

The structure was refined, first with isotropic and then with anisotropic temperature factors for non-hydrogen atoms, to an R of 0.071. Since all the protons could not be located from the difference Fourier map, the structure was further refined, using calculated hydrogen positions, to the final R of 0.048. The scattering factors used were those of Cromer et al.[15] The final atomic coordinates for non-hydrogen atoms are given in Table I.

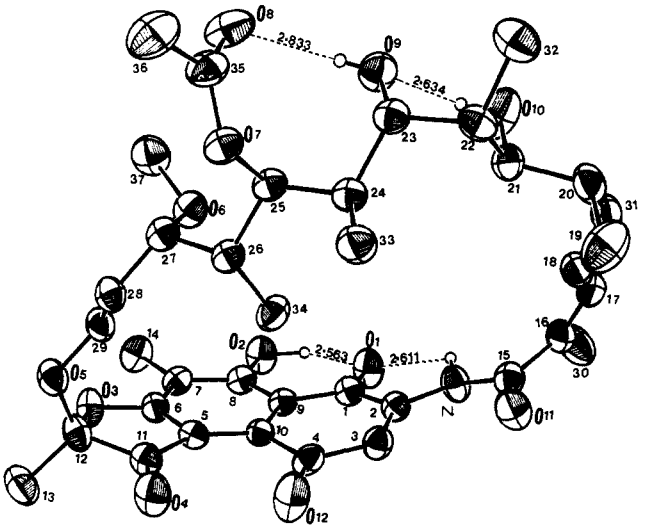

Figure 1. Thermal ellipsoid plot of the molecule. Intramolecular hydrogen bonds are depicted by dashed bonds.

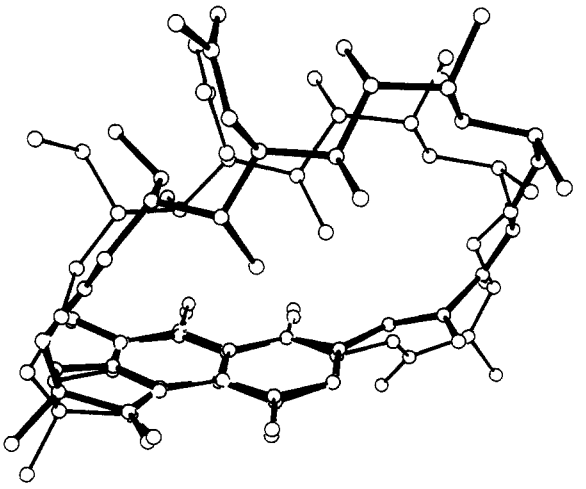

Figure 2. Comparison of conformation of rifamycin S and rifamycin (thin bonds). The 3-formylhydrazone of rifampicin has been omitted for the sake of clarity.

Results and Discussion

Geometry. The average standard deviations in the bond distances and angles are of the order of 0.006–0.01 Å and 0.4–0.6°, respectively. The bond distances and angles in the naphthoquinone part agree very well with those in substituted rifamycin S molecules, e.g., 3-carbomethoxyrifamycin S (CMRS)[12] and rifamycin S iminoethyl ether.[9] The biggest difference from CMRS is 0.041 Å in the bond length C(3)–C(4). This is expected because CMRS is a

(1) Sensi, P.; Furesz, S.; Maffii, G. *Antimicrob. Agents Chemother.* **1966**, 699–705.
(2) Joss, U. R.; Hughes, A. M.; Calvin, H. *Nature (London)* **1973**, *242*, 88–90.
(3) Hartmann, G. K.; Honikel, O.; Knusel, F.; Nuesch, J. *Biochim. Biophys. Acta* **1967**, *145*, 843–844.
(4) Umezawa, H.; Mizuno, S.; Yamazaki, H.; Nitta, K. *J. Antibiot.* **1968**, *21*, 234–236.
(5) Brufani, M.; Cerrini, S.; Fideli, W.; Vaciago, A. *J. Mol. Biol.* **1974**, *87*, 409–435.
(6) Brufani, M. *Top. Antibiot.* **1977**, *1*, 91–212.
(7) Lancini, G.; Zanchelli, W. "Structure-Activity Relationship Among Semisynthetic Antibiotics"; Perlman, D., Ed.; Academic Press: New York, 1977; pp 531–600.
(8) Arora, S. K. *Mol. Pharmacol.* **1983**, *23*, 133–140.
(9) Arora, S. K. *Acta Crystallogr.* **1981**, *37*, 152–157.
(10) Arora, S. K.; Main, P. *J. Antibiot.*, in press.
(11) Gadret, M.; Gourselle, M.; Liger, J. M.; Colleter, J. C. *Acta Crystallogr., Sect. B.: Struct. Crystallogr. Cryst. Chem.* **1975**, *B31*, 1454–1462.
(12) Brufani, M.; Cellai, L.; Cerrini, S.; Fideli, W.; Segree, A.; Vaciago, A. *Mol. Pharmacol.* **1982**, *21*, 394–399.
(13) Brufani, M.; Cellai, L.; Cerrini, S.; Fideli, W.; Vaciago, A. *Mol. Pharmacol.* **1978**, *14*, 693–703.
(14) Germain, G.; Main, P.; Woolfson, M. M. *Acta. Crystallogr., Sect. A.: Cryst. Phys., Diffr., Theor. Gen. Crystallogr.* **1971**, *A27*, 368–376.
(15) Cromer, D. T.; Mann, J. B. *Acta Crystallogr., Sect. A: Cryst. Phys., Diffr., Theor. Gen. Crystallogr.* **1968**, *A24*, 321–324.

Table I. Atomic Positions and Equivalent Isotropic Thermal Parameters

atom	x	y	z	U, Å²
O(1)	0.8201 (3)	0.0897 (3)	0.6175 (2)	0.070 (2)
O(2)	0.6248 (3)	0.0769 (3)	0.6068 (2)	0.068 (2)
O(3)	0.4835 (2)	0.1306 (3)	0.4008 (2)	0.0567 (12)
O(4)	0.6845 (3)	0.2196 (3)	0.3065 (2)	0.077 (2)
O(5)	0.5223 (3)	0.0701 (3)	0.2986 (2)	0.0577 (12)
O(6)	0.7025 (3)	−0.1536 (3)	0.3619 (2)	0.0565 (13)
O(7)	0.8737 (3)	−0.2340 (2)	0.22647 (15)	0.0529 (12)
O(8)	0.8451 (4)	−0.3748 (3)	0.2720 (2)	0.083 (2)
O(9)	1.0092 (4)	−0.3275 (3)	0.3559 (2)	0.066 (2)
O(10)	1.1386 (4)	−0.2799 (4)	0.4486 (2)	0.085 (2)
O(11)	1.1418 (3)	0.1152 (3)	0.5022 (2)	0.076 (2)
O(12)	0.8570 (3)	0.2290 (4)	0.3810 (2)	0.098 (2)
O(W1)	0.2331 (5)	0.4121 (4)	0.0097 (3)	0.121 (2)
O(W2)	0.0220 (11)	0.3835 (11)	−0.0157 (7)	0.160 (5)
N	1.0063 (4)	0.0972 (4)	0.5700 (2)	0.059 (2)
C(1)	0.8251 (4)	0.1155 (4)	0.5597 (2)	0.048 (2)
C(2)	0.9278 (4)	0.1280 (4)	0.5305 (2)	0.048 (2)
C(3)	0.9368 (4)	0.1682 (4)	0.4718 (2)	0.054 (2)
C(4)	0.8469 (4)	0.1903 (4)	0.4325 (2)	0.052 (2)
C(5)	0.6557 (4)	0.1641 (3)	0.4182 (2)	0.044 (2)
C(6)	0.5628 (4)	0.1345 (3)	0.4444 (2)	0.046 (2)
C(7)	0.5476 (4)	0.1058 (3)	0.5075 (2)	0.047 (2)
C(8)	0.6365 (4)	0.1059 (4)	0.5454 (2)	0.047 (2)
C(9)	0.7330 (4)	0.1303 (3)	0.5208 (2)	0.043 (2)
C(10)	0.7429 (4)	0.1628 (3))	0.4566 (2)	0.0417 (15)
C(11)	0.6338 (4)	0.1852 (4)	0.3490 (2)	0.052 (2)
C(12)	0.5233 (4)	0.1525 (4)	0.3370 (2)	0.055 (2)
C(13)	0.4569 (5)	0.2208 (4)	0.3034 (3)	0.073 (2)
C(14)	0.4459 (4)	0.0727 (5)	0.5319 (3)	0.067 (2)
C(15)	1.1077 (4)	0.0821 (4)	0.5516 (3)	0.056 (2)
C(16)	1.1677 (4)	0.0244 (4)	0.5977 (3)	0.057 (2)
C(17)	1.2252 (4)	−0.0460 (4)	0.5756 (3)	0.058 (2)
C(18)	1.2335 (4)	−0.0787 (4)	0.5086 (3)	0.057 (2)
C(19)	1.2839 (4)	−0.1532 (4)	0.4914 (3)	0.062 (2)
C(20)	1.2889 (4)	−0.1926 (4)	0.4225 (3)	0.062 (2)
C(21)	1.1801 (4)	−0.2180 (4)	0.4008 (2)	0.053 (2)
C(22)	1.1734 (4)	−0.2637 (4)	0.3322 (2)	0.053 (2)
C(23)	1.0623 (4)	−0.2714 (4)	0.3094 (2)	0.051 (2)
C(24)	1.0084 (4)	−0.1769 (3)	0.2985 (2)	0.046 (2)
C(25)	0.8929 (4)	−0.1877 (3)	0.2893 (2)	0.045 (2)
C(26)	0.8292 (4)	−0.0989 (3)	0.2870 (2)	0.046 (2)
C(27)	0.7157 (4)	−0.1240 (4)	0.2963 (2)	0.048 (2)
C(28)	0.6450 (4)	−0.0463 (4)	0.2779 (2)	0.049 (2)
C(29)	0.5866 (4)	−0.0009 (4)	0.3193 (3)	0.052 (2)
C(30)	1.1583 (6)	0.0452 (3)	0.6696 (3)	0.092 (3)
C(31)	1.3363 (6)	−0.1179 (6)	0.3760 (4)	0.098 (3)
C(32)	1.2274 (6)	−0.3585 (4)	0.3291 (3)	0.079 (2)
C(33)	1.0587 (4)	−0.1216 (4)	0.2431 (3)	0.063 (2)
C(34)	0.8628 (4)	−0.0241 (4)	0.3358 (3)	0.059 (2)
C(35)	0.8515 (5)	−0.3239 (4)	0.2251 (3)	0.062 (2)
C(36)	0.8327 (6)	−0.3568 (5)	0.1566 (3)	0.091 (3)
C(37)	0.6261 (5)	−0.2236 (4)	0.3717 (3)	0.074 (2)

3-substituted rifamycin S. The bond distances and angles in the *ansa* chain part of the molecule again are in good agreement with other rifamycins.

Conformation. The stereochemistry of the rifamycin S molecule, as shown in Figure 1, approximately resembles that of its reduced form, rifamycin SV. The differences are in the dihedral angles between the naphthoquinone nucleus and the five-membered ring attached to it (12 and 8°) and also in the orientation of the *ansa* chain with respect to the naphthoquinone plane (114 and 75°).

Figure 2 compares the conformations of RIFAS and RIFAMP. The torsion angles C(1)–C(2)–N–C(15) and N–C(15)–C(16)–C(17) have values of 166 and 133° in RIFAS, whereas these values in RIFAMP and RIFAB are −32, −43, −55, and −31°, respectively. These differences reflect the reversal of amide and carbonyl groups. The torsion angle C(28)–C(29)–O(5)–C(12) at the other junction, C(12), has a value of −136° in RIFAS which is closer to those of RIFASV (−178°) and CMRS (−127°) but farther from those of RIFAMP (65°) and RIFAB (49°). Thus, although the middle part of the *ansa* chain appears to be relatively rigid, the *ansa* bridge seems to rock as a unit about its joining points with the chromophore.

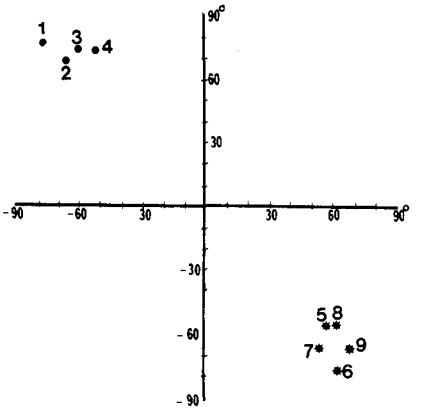

Figure 3. Preferred values for torsion angles C(21)–C(22)–C(23)–C(24) and C(29)–O(5)–C(12)–O(3) for active (RIFAS (5), RIFAmP (6), RIFAB (7), RIFASV (8), CMRS (9)) and inactive (cyclized rifamycin SV (1, 2), rifamycins iminomethyl ether (3, 4)) rifamycins.

Table II. Comparison between the the Dihedral Angle Values Obtained by ^{1}H NMR and X-rays for Rifamycin S

dihedral angle	NMR[18]	X-ray[a]
H(17)–C(17)–C(18)–H(18)	160	−173
H(19)–C(19)–C(20)–H(20)	32	0
H(20)–C(20)–C(21)–H(21)	175	−172
H(21)–C(21)–C(22)–H(22)	80	65
H(22)–C(22)–C(23)–H(23)	52	63
H(23)–C(23)–C(24)–H(24)	−175	−170
H(24)–C(24)–C(25)–H(25)	−54	−62
H(25)–C(25)–C(26)–H(26)	175	−168
H(26)–C(26)–C(27)–H(27)	50	68
H(27)–C(27)–C(27)–H(28)	150	−179

[a] From calculated geometrical positions of hydrogen.

While scanning through the torsion angles along the *ansa* chain of active and inactive rifamycins, one observes an interesting feature, i.e., in all the rifamycins that have activity against DDRP (RIFAS, RIFASV, RIFAMP, RIFAB, CMRS), the torsion angle C(21)–C(22)–C(23)–C(24) has values in the range 59 ± 6°, while in inactive rifamycins (CYRIFASV, RIFASIME) the values are in the range −60 ± 12°. Similar results are observed for the torsion angle C(29)–O(5)–C(12)–O(3), where the values are −65 ± 13 and 65 ± 13° for active and inactive rifamycins. One could say that these angles have preferred values. Figure 3 shows the interrelationship between these two angles.

Several NMR studies on the solution conformation of rifamycin S, as well as on the effect of the 3-substitution on the conformation of the *ansa* chain, have been done.[16-18] Table II gives the comparison of the dihedral angles calculated from coupling constants (NMR spectra in D_2O and $CDCl_3$)[18] and from X-ray diffraction. One observes some differences in dihedral angles H(17)–C(17)–C(18)–H(18), H(20)–C(20)–C(21)–H(21), and H(27)–C(27)–C(28)–H(28). The difference in the H(17)–C(17)–C(18)–H(18) dihedral angle values (27°) can be attributed to its being in the vicinity of the carbonyl group, which can have different

(16) Gallo, G. G.; Martinelli, E.; Pagani, V.; Sensi, P. *Tetrahedron* **1974**, *30*, 3093–3097.
(17) Casey, M. L.; Whitlock, M. W. *J. Am. Chem. Soc.* **1975**, *97*, 6231–6236.
(18) Cellai, L.; Cerrini, S.; Segre, A.; Brufani, M.; Fideli, W.; Vaciago, A. *J. Org. Chem.* **1982**, *47*, 2652–2661.

Table III. Distances (Å) between O(1), O(2), O(9), and O(10) in RIFAS, RIFASV, RIFAMP, RIFAB, CMRS, RIFASIME, TOLYPO, and CYRIFASV

atoms	RIFAS	RIFASV	RIFAMP	RIFAB	CMRS	RIFASIME	TOLYPO	CYRIFASV
O(1)–O(2)	2.6	2.5	2.5	2.6	2.5	2.5	2.5	2.6
O(1)–O(9)	8.1	7.5	6.2	6.7	7.0	6.2	3.2	5.2
O(1)–O(10)	7.5	6.7	5.4	5.7	5.8	4.1	3.0	4.0
O(2)–O(9)	9.2	8.3	6.8	7.8	7.4	4.7	3.3	4.3
O(2)–O(10)	9.0	8.1	6.9	7.5	7.0	3.8	4.8	3.9
O(9)–O(10)	2.6	2.6	2.7	2.7	2.7	2.	2.6	2.6

orientations in solution and solid state. But overall, the conformations in solid state and solution are the same.

Packing and Hydrogen Bonding. The intramolecular hydrogen bonds with the distances are shown in Figure 1. The intermolecular hydrogen bonds (Å) are OW(1)→O(10) = 2.809 ($2 - X$, $^1/_2 + y$, $^3/_2 - z$), OW(1)→O(6) = 2.926 ($^3/_2 - x$, y, $^1/_2 - z$), and OW(2)→OW(1) = 2.878 ($^3/_2 - x$, $1 - y$, $-^1/_2 - z$).

Structure–Activity. Dampier and Whitlock[19] correlated the effect of the 3-substitution on the activity of rifamycin S. Their studies indicated that the higher the electronegativity of the substituent at the 3-position, the more the activity of rifamycin toward DDRP. One effect of having an electron donor group at the 3-position is to reorient the amide group so that it forms a hydrogen bond with the substituent. This will rotate the carbonyl group to the inward direction. This effect is also observed in the solid state, e.g. rifampicin, which is a 3-formylhydrazone (strongly electronegative) derivative of rifamycin SV and has a conformation where the C=O is rotated toward the inside of *ansa* chain by 138°, while in the case of 3-carbomethoxy (very little electronegative character) rifamycin S the angle of rotation is only 53°.

Previous studies[8,9,12] have demonstrated that the activity of rifamycins is dependent upon (a) the type (I or II)[8] of conformation at the junction of the chromophore with the *ansa* chain at C(2) and C(12) and (b) the spatial arrangement of oxygent atoms O(1), O(2), O(9), and O(10). The results of the present study do not contradict above correlations. Table III compares the spatial distances between the above oxygen atoms in rifamycin S and in other active and inactive[9,12,13] rifamycins.

It has been indicated from previous biochemical studies[20–22] that (1) π–π (or stacking) interactions (between naphthoquinone or hydroquinone and aromatic amino acids of β-unit of enzyme DDRP) and hydrogen bonding are involved in the formation of antibiotic–enzyme complexes, (2) DNA-dependent RNA polymerase is a metalloenzyme, i.e., it contains two atoms of Zn per DDRP molecule, (3) rifamycins bind metal atoms, and (4) our space-filling models indicate that active rifamycins prefer to attach to the β-sheet rather than the α-helix part of DDRP (due to steric hindrance).

From the available information, one can speculate a four-step model for the interaction of rifamycins with DNA-dependent RNA polymerase: (a) Rifamycin binds to the zinc atom of DDRP through O(1) and O(2). (b) An atomatic amino acid (tyrosine or phenyl alanine or tryptophan) of the enzyme stacks with chromophore of rifamycin (preliminary NMR studies in this laboratory on rifamycin S and phenylalanine give indications of stacking). (c) The middle part of the *ansa* chain lines up with the β-sheet part of the enzyme. (d) O(9) and O(10) form strong hydrogen bonds with electronegative groups on the enzyme. The complexity of the DDRP molecule (MW 500 000 Da) makes it almost impossible to study the three-dimensional structure of antibiotic–DDRP complex at this stage.

Acknowledgment. The author is indebted to the Natioanl Institutes of Health (Grant GM 32690) for financial support. The author also thanks Dr. S. Larson for help with the project.

Registry No. DDRP, 9014-24-8; RIFAS·2H_2O, 96914-15-7; RIFAMP, 13292-46-1; RIFAB, 13232-69-4; RIFASV, 6998-60-3; CMRS, 72393-97-6; TOLYPO, 22356-23-6; RIFASIME, 14768-65-1; RIFAS, 13553-79-2; CYRIFASV, 90817-36-0; ansamycin, 51374-14-2.

Supplementary Material Available: Listings of bond lengths, angles, thermal parameters, hydrogen coordinates, structure factor tables, and torsion angles (25 pages). Ordering information is given on any current masthead page.

(19) Dampier, M. F.; Whitlock, M. W., Jr. *J. Am. Chem. Soc.* **1975**, *197*, 6254–6256.
(20) Wyss, W.; Wherli, W. *Experientia* **1973**, *29*, 760–767.
(21) Scrutton, M. C.; Wu, C. W.; Goldthwait, D. A. *Proc. Natl. Acad. Sci. U.S.A.* **1971**, *2497*–2501.
(22) Kono, Y.; Sugiuara, Y. *J. Biochem.* **1982**, *91*, 397–401.